FINAL REPORT

TO: NATIONAL AERONAUTICS AND SPACE ADMINISTRATION
AMES RESEARCH CENTER

FROM: NORTH CAROLINA STATE UNIVERSITY
RALEIGH, N.C. 27695-7905

FOR: "HETEROGENEOUS PHOTOCATALYTIC OXIDATION OF
ATMOSPHERIC TRACE CONTAMINANTS"
NASA RESEARCH GRANT 2-684

PRINCIPAL INVESTIGATOR: DAVID F. OLLIS
CHEMICAL ENGINEERING DEPARTMENT
NORTH CAROLINA STATE UNIVERSITY
RALEIGH, NC. 27695-7905
PHONE: 919-515-2329
FAX: 919-515-3465
ollis@che.ncsu.edu

PERIOD COVERED: 11/1/90-9/30/96

MAR 1 4 1997

CC: CASI

TABLE OF CONTENTS

1. INTRODUCTION

Heterogeneous photocatalysis involves the use of a light-activated catalyst at room temperature in order to carry out a desired reaction. In the presence of molecular oxygen, illumination of the n-type semiconductor oxide titanium dioxide ($TiO2$) provides for production of highly active forms of oxygen, such as hydroxyl radicals, which are able to carry out the complete oxidative destruction of simple hydrocarbons such as methane, ethane, ethylene, propylene, and carbon monoxide.

This broad oxidation potential, coupled with the ability with sufficient residence time to achieve complete oxidation of simple hydrocarbon contaminants to carbon dioxide and water, indicated that heterogeneous photocatalysis should be examined for its potential for purification of spacecraft air. If a successful catalyst and photoreactor could be demonstrated at the laboratory level, such results would allow consideration of photocatalysts as a partial or complete replacement of adsorption systems, thereby allowing for reduction in lift-off weight of a portion of the life support system for the spacecraft, or other related application such as a space station or a conventional commercial aircraft.

The present research was undertaken to explore this potential through achievement of the folowing plan of work:

(a) ascertain the intrinsic kinetics of conversion of pollutants of interest in spacecraft,

(b) ascertain the expected lifetime of catalysts through examination of most likely routes of catalyst deactivation and regeneration

(c) model and explore experimentally the low pressure drop catalytic monolith, a commercial configuration for automotive exhaust control

1

(d) examine the kinetics of multicomponent conversions.

In the recent course of this work, we have also discovered how to increase catalyst activity via halide promotion which has allowed us to achieve approximately 100% conversion of an aromatic contaminant (toluene) in a very short residence time of 5-6 milliseconds.

Conclusions apper in section 8 below.

2.   THE SPACECRAFT ATMOSPHERE

The contaminants in the atmosphere of an enclosed, isolated spacecraft are determined by outgassing and evaporation from the materials and inhabitants present.   An illustrative list of the contaminat types, daily production rates, and spacecraft maximum allowable levels for each of a number of expected contaminants was presented by Leban and Wagner.   This list formed the basis for the reactant classes we considered (alcohol, aldehyde, aromatic, etc.), and that compound in each class which was generated at the highest rate suggested the key compound from that class for this scoping study to establish the potential of photocatalysis for the purification of multiply contaminated spacecraft air.   Examples in this latter category included   acetone (ketone class), 1-butanol (alcohol class), and m-xylene (aromatic class), all of which we examined and report upon in the following pages.

The role of water vapor is also examined and found important. Previous literature indicated a variable influence of water vapor in concentrations from 0% to as high as 100 % relative humidity, the latter corresponding to about 3 volume percent in air at ambient temperature.   For example,   water vapor enhances the rate of disappearance of 80 parts per million (ppm) toluene up to the highest value examined, 60 % relative humidity (about 20,000 ppm) (Ibusuki et al (1985)), but inhibits trichloroethylene conversion above just 1% (Dibble and Raupp (1988, 1990).   We found reactant-specific results as well: water vapor enhances m-xylene conversion at low concentrations, but inhibits it mildly at higher

2

levels, it has no influence on the rate of n-butanol conversions, and it inhibits acetone conversion. Thus, the influence of 30-60% relative humidity , appropriate for human comfort, on photocatalyst activity requires investigation for each contaminant of interest.

The lifetime of a catalyst is determined by the concentration and indentity of the most strongly deactivating contaminants. Expected air contaminants containing either nitrogen or silicon are shown to deactivate photocatalysts appreciably, while the sulfur containing dimethylsulfide had almost no effect (Peral and Ollis (1993)).

3. PHOTOCATALYTIC DESTRUCTION KINETICS

Knowledge of the intrinsic kinetics of a chemical reaction is a prerequisite to reactor design and system optimization. With reaction kinetics codified as a reaction rate equation, the engineer can ascertain how the reaction rate will change as a function of feed composition. The rate equation can be combined with appropriate balance equations to predict the performance of various reactor configurations and the importance of mass transfer and other influences, especially intensity variations in the present study, on the global efficiency of pollutant removal and destruction.

Our kinetic studies examined four topics, all appropriate to the NASA spacecraft atmosphere, and all relatively lacking in the previous literature: (a) conversion kinetics for oxygen-containing contaminants, (b) conversion of aromatics , (c) conversion of oxyhydrocarbon contaminants containing heteroatoms, e.g, sulfur, nitrogen, and silicon, and (d) kinetics of multicomponent conversions, appropriate to multiply contaminated air as is expected in spacecraft.

We demonstrate, in the subsequent photocatalytic monolith reactor design section, the use of our rate equations (for acetone and butanol, as illustrative examples of slow and moderately rapid conversions).

3

The multicomponent conversion kinetics are explored in two studies. In the first, the sequential conversion of ethanol, and of all its intermediates (acetaldehyde, formaldehyde, and formic acid) on the pathway to carbon dioxide and water, provides an example of the influence of competitive consumption of active oxygen and surface sites by the various reactive species. The second, an exploration of simultaneous conversion of toluene and trichloroethylene, reveals a new approach to obtain approximately 100% conversion of one reactant (toluene), presumably by entraining it in the rapid chain reaction oxidation involving chlorine atoms from the second reactant (trichloroethylene).

Finally, the influence of intensity of photocatalytic kinetics is explored in three ways: (a) acetone conversion kinetics, (b) monolith design with axial illumination, and (c) direct measurements of the monolith illumination field.

A. OXYGENATES: ACETONE, BUTANOL, BUTERALDEHYDE AND FORMALDEHYDE

Conversion of trace levels of acetone, butanol (and its intermediate buteraldehyde), and formaldehyde was studied for each reactant in a downflow powder layer reactor (Peral and Ollis (1992)) designed to avoid any mass transfer influence and hence to provide a direct measure of intrinsic kinetics of conversion.

The catalyst activity is routinely high enough that appreciable conversion takes place during the single downward passage of contaminated air through the top-illuminated powder layer. With sufficient catalyst powder present to guarantee complete light absorption, the rate equation, presumed to be of the Langmuir-Hinshelwood form, can be combined with the Lamber-Beer law to give the differential mass balance on contaminant, equation (1):

$$v \, (dC/dz) = - k_o \, e^{-\beta \mu z} \, K \, C \, / \, (1. + K \, C) \qquad (1)$$

where k_o, β, μ, K, v, and C are respectively the catalytic rate constant, the fractional dependence on intensity (=.7), the light

4

absorption coefficient of titania, the reactant binding constant, the air flow velocity, and the contaminant concentration.

Integration and rerrangement provides equation (2) which indicates that a plot of ln (C/Co) / (C-Co) vs. 1. / (C-Co) will be a straight line if the Langmuir-Hinshelwood assumption was correct.

$$\frac{\ln (C / Co)}{(C - Co)} = - \frac{ko\,K}{\beta\,\mu\,v} \cdot \frac{1}{(C - Co)} - K \qquad (2)$$

Figures 1 (acetone) and 2 (butanol) on the following page demonstrate that this convenient kinetic representation of integral conversion data provides a satisfactory approach for determining the Langmuir-Hinshelwood rate parameters.
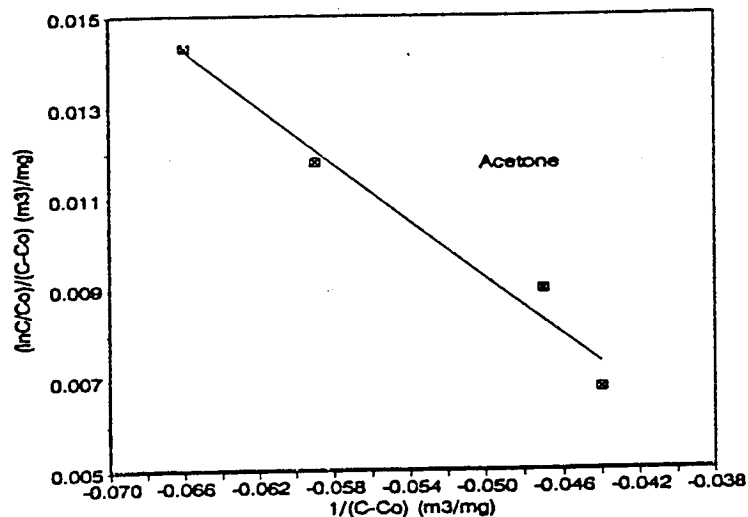

FIG. 1 Plot of $(C - C_0)^{-1} \cdot \ln(C/C^0)$ vs $(C - C_0)^{-1}$ for acetone data in Table 1. $I_a = 3.5 \times 10^{-7}$ Einstein/ $cm_2 \cdot$ min (200-W high-pressure Hg–Xe lamp); $T = 22$–$24°C$.
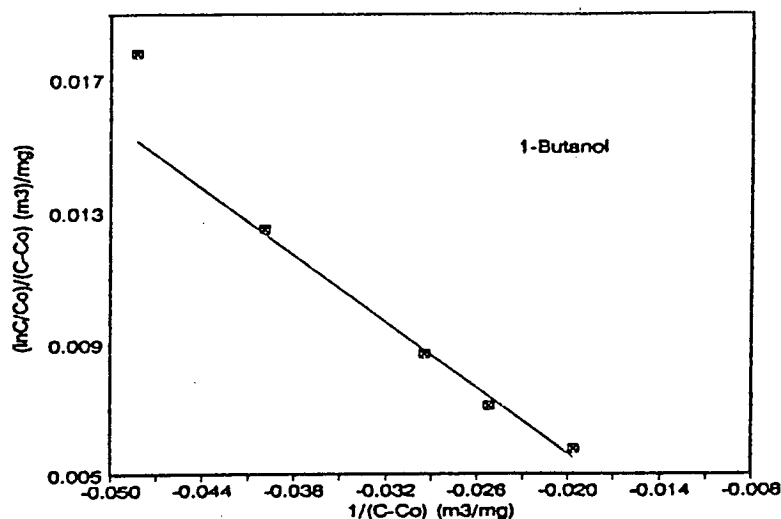
5

FIG. 2 · Plot of $(C - C_0)^{-1} \cdot \ln(C/C^0)$ vs $(C - C_0)^{-1}$ for 1-butanol data in Table 1. $I_a = 5.0 \times 10^{-7}$ Einstein/$cm^2 \cdot min$ (100-W blacklight); T = 22–24°C.

The influence of intensity on the rate of photocatalyzed reactions is important in two respects. Fundamentally, early work from the paint pigment industry established that photocatalytic reaction rates would vary as intensity to the first power at very low light levels, and as intensity to the 0.5 power at high light levels. These exponents reflect the two asymptotes of high quantum yield (every photoproduced excitation converts one molecule) to low quantum yield (high photogeneration rate of electrons (e⁻) and holes(h⁺) leads to excessive electron-hole recombination and inefficiency.)

A plot of the logarithm of rate of acetone conversion vs. the top surface irradiance (Figure 3) establishes that for our moderate illumination levels, the rate varies as the 0.7 power of intensity. This rate dependence was used in our subsequent monolith modelling section for both acetone and butanol calculations.

The process economics of photocatalytic conversions depend in part on the quantum efficiency, i.e, the number of molecules reacted per photon absorbed by the catalyst. Ferrioxalate actinometry was used to measure the absolute photon flux ariving at the top of the
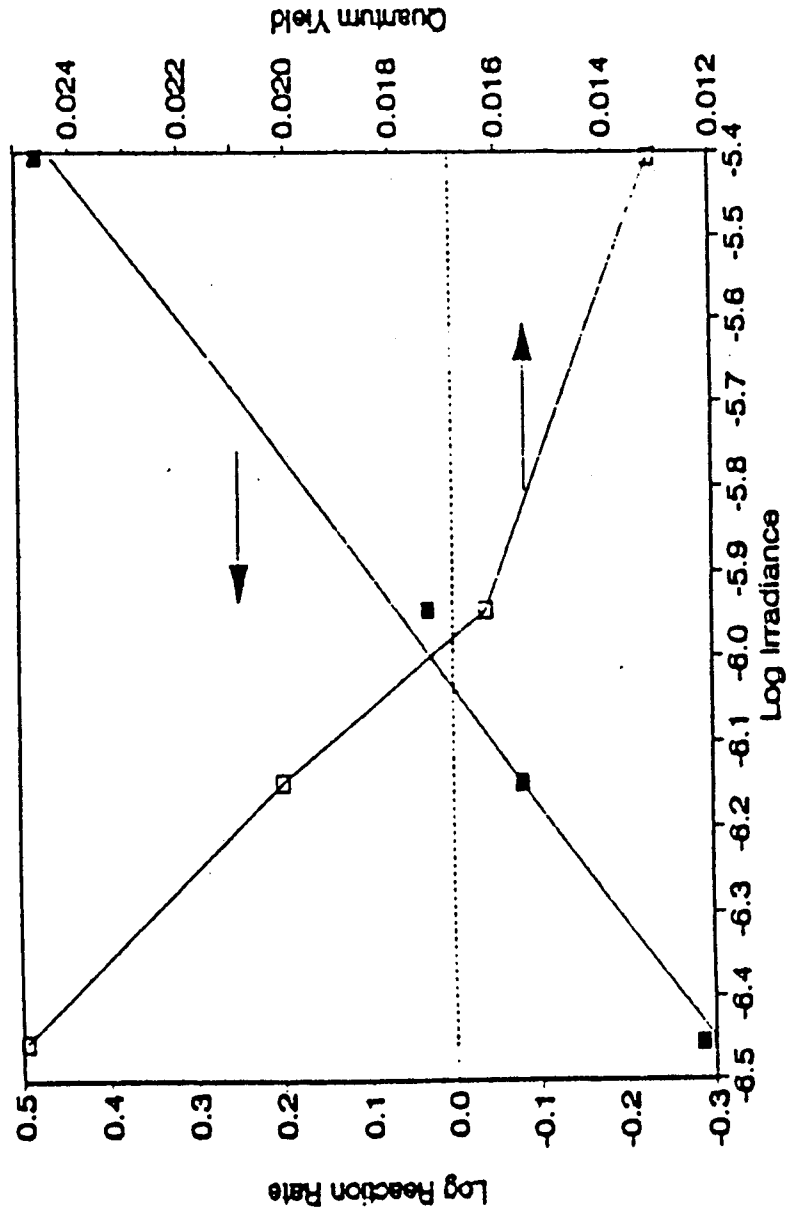
6

FIG. 3. Reaction rate of acetone photooxidation and quantum yield vs irradiance. $[Acetone]_0 = 160$ mg/m^3; $T = 22$–$24°C$. Reaction rate and irradiance units are $\mu g/cm^2 \cdot min$ and $Einstein/cm^2 \cdot min$, respectively.

catalyst powder layer. The calculated quantum efficiency is between 1.3 and 2.5%, as shown in Figure 3.

Water is itself an oxygenate, and may compete for surface binding sites and accelerate or inhibit the individual reaction rates. Figures 4 and 5 show that water had no effect on alcohol conversion rate, but did exhibit an inhibition effect on acetone conversion. This latter inhibition could be represented by equation (3) :

$$\text{rate (with water)} = \frac{\underline{\text{rate (without water)}}}{1. + K_{H2O} \ (H2O)^{\Omega}} \qquad (3)$$

where K and Ω are constants. This water vapor dependence can be used to model variations in relative humidity for acetone conversion.
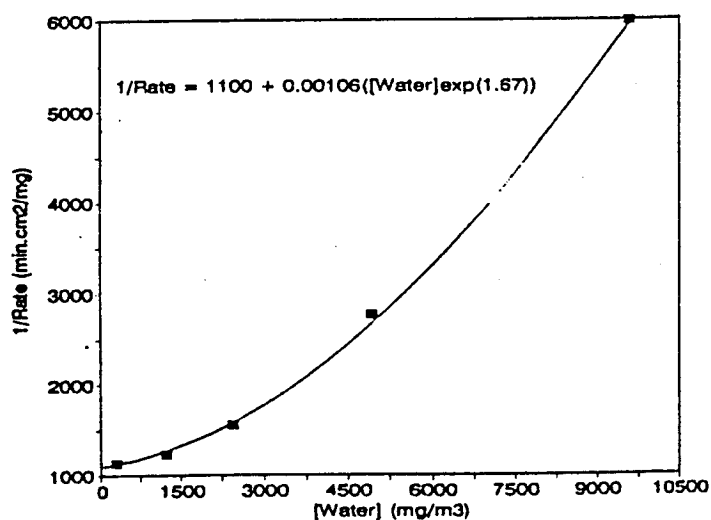

FIG. 4 Inverse of reaction rate of acetone photooxidation vs water concentration in the gas phase. [Acetone]$_0$ = 200 mg/m^3; T = 22–24°C. 200-W high-pressure Hg–Xe lamp. Reaction rate and water concentration units are mg/cm$^2 \cdot$ min and mg/m^3, respectively.
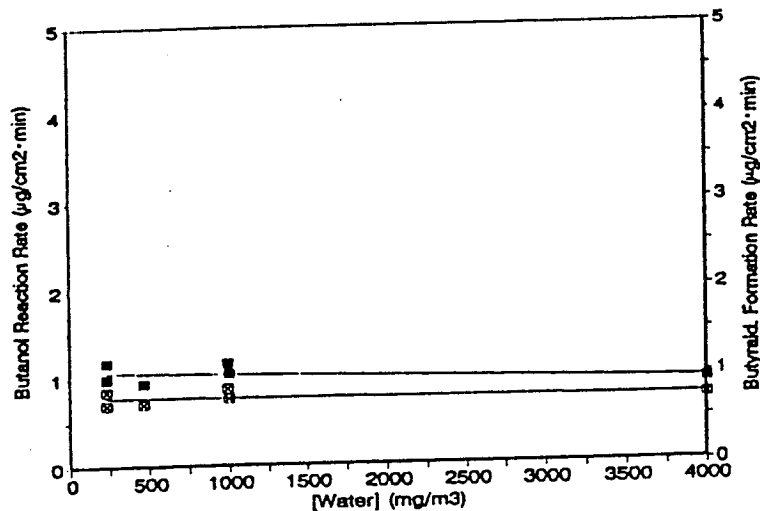
FIG. 5. Reaction rate of 1-butanol photooxidation and butyraldehyde formation vs water concentration in the gas phase. $I_a = 5.0 \times 10^{-7}$ Einstein/cm^2 · min (100-W blacklight); $T = 22–24°C$.

B. AROMATICS: m-XYLENE

Aromatics apear on the expected spacecraft contaminant list, with meta-xylene being the most prevalent. Prior literature with aromatics is extremely sparse. Ibusuki et al (1985) examined the photocatalyzed attack of toluene at 80 ppm in dry and in humidified air. They found a very low rate of reaction in dry air, and observed that the conversion obtained after 10 minutes of reaction time

8

increased linearly with the relative humidity of the feed air up to 60% , the largest value examined. Only a trace of benzaldehyde was observed as a reaction intermediate, always at less than 1 ppm. This lack of appreciable gas phase intermediates is a desirable process characteristic; carbon dioxide was the overwhelming single product observed by these investigators.

In our examination of m-xylene conversion in the powder bed reactor, the reaction rate was again reasonably described by Langmuir-Hinshelwood kinetics, as indicated by the linear plot in Figure 6. No reaction intermediates were detected with our gas chormatograph/flame ionization detector; thus, m-xylene conversion appears to be relatively clean, just as found previously for toluene by Ibusuki et al (1985).

The influence of water on m-xylene conversion is different from Ibusuki's 1985 work with toluene. We find that small additions of water do increase the catalyst activity up to 60% vs. the dry air value, but further humidification leads to a depression of xylene conversion rate, as shown in Figure 7.

In summary, we find from our kinetic studies the following results useful for subsequent reactor design:

(i) the Langmuir-Hinshelwood rate form usefully represents the rate vs. concentration dependence for oxygenates and aromatics

(ii) the rate varies as the 0.7 power of the local light intensity

(iii) the rate varies with relative humidity in a fashion specific to each individual reactant: activating toluene conversion, and m-xylene as well at low humidities; inhibiting acetone conversion, and m-xylene at high humidities; and having no influence on butanol conversion.

(iv) the powder layer reactor provides a simple, convenient configuration for measurement of rates without the confounding influence of mass transfer or other physical process influences.
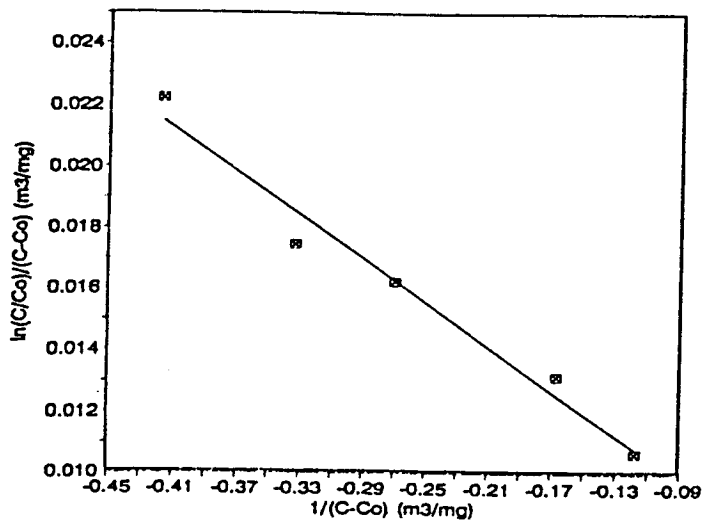
FIG. 6   Plot of $(C - C_0)^{-1} \cdot \ln(C/C^0)$ vs $(C - C_0)^{-1}$ for m-xylene data in Table 1. $I_a = 5.0 \times 10^{-7}$ Einstein/ $cm^2 \cdot$ min (100-W blacklight); $T = 22–24°C$.
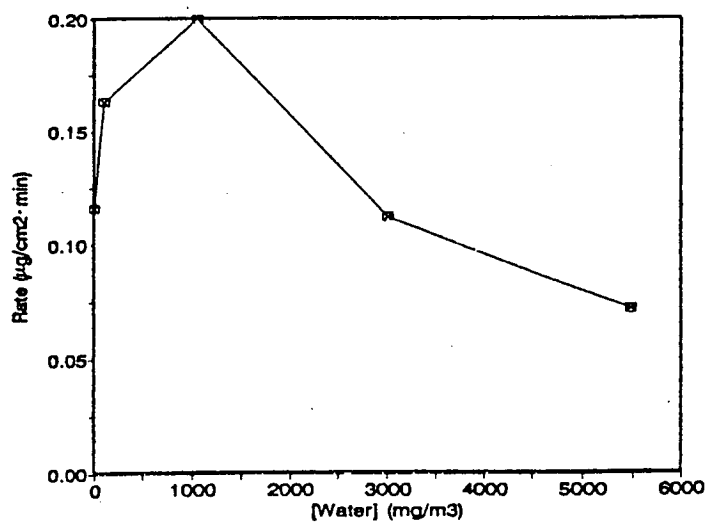

FIG. 7   Reaction rate of m-xylene photooxidation ·s water concentration in the gas phase. $I_a = 5.0 \times 10^{-7}$ Einstein/$cm^2 \cdot$ min (100-W blacklight); $T = 22–24°C$.

10

C. HETEROATOM CONTAMINANTS:

Total oxidation of sulfur-, nitrogen-, or silicon-containing molecules would be expected to yield, in addition to water and carbon dioxide, oxidized forms of the heteroatoms, e.g, sulfate, nitrate, silicate, etc. These high oxidation species are not volatile and may be expected to deposit on the catalyst, leading to accumulation and possible catalyst deactivation. Thus, study of photocatalytic removal of air contaminants containing such heteroatoms is important both from a rate-of-removal viewpoint and from an interest in catalyst lifetime and catalyst deactivation and reactivation.

1. NITROGEN: PYRROLE, INDOLE

Indole and pyrrole (methyl-indole) are aromatic structures containing nitrogen; these two compounds appear on the Leban and Wagner list as the most common nitrogen-containing hydrocarbons. Photocatalytic conversion of each N-aromatic was studied in the powder flow reactor.

With a pyrrole/air feed, a 60% initial conversion was recorded; this value declined steadily with time. A log-log plot of rate vs. time was linear, as shown in Figure 8. With pyrrole, the activity disappeared completely after 400 minutes. The amount of pyrrole or indole reacted at which activity was lost corresponded to only several monolayer equivalents on the catalyst surface. Illumination in fresh, contaminant free air did not recover catalyst activity, in contrast to our earlier findings with the slow deactivation induced by butanol.

In order to examine the surface composition of a deactivated catalyst, Auger spectra were taken. These spectra show only titanium and oxygen on a fresh catalyst. However, a deactivated catalyst displays major additional peaks for nitrogen and carbon

11

(Figure 9), implying the accumulation not only of N but of substantial carbonaceous species of unknown structures. Similar results were obtained with indole.
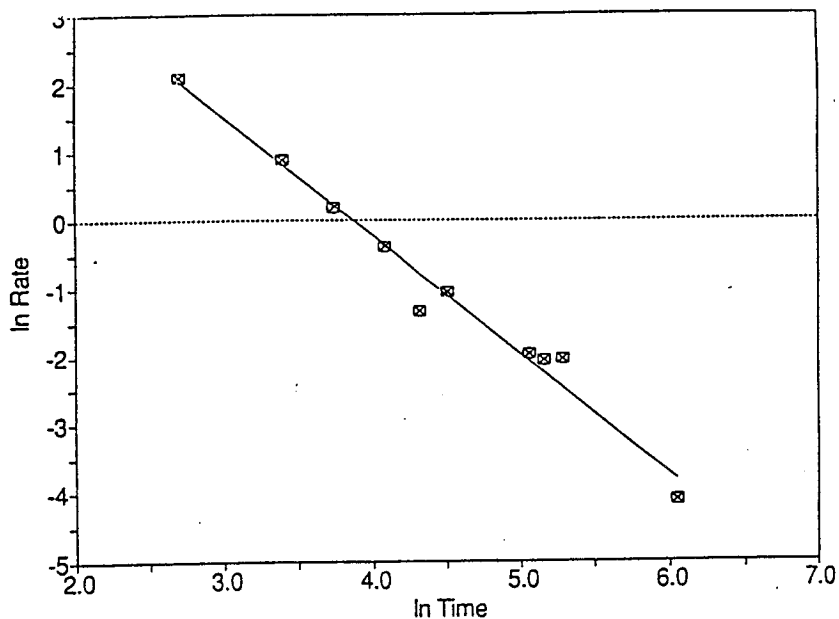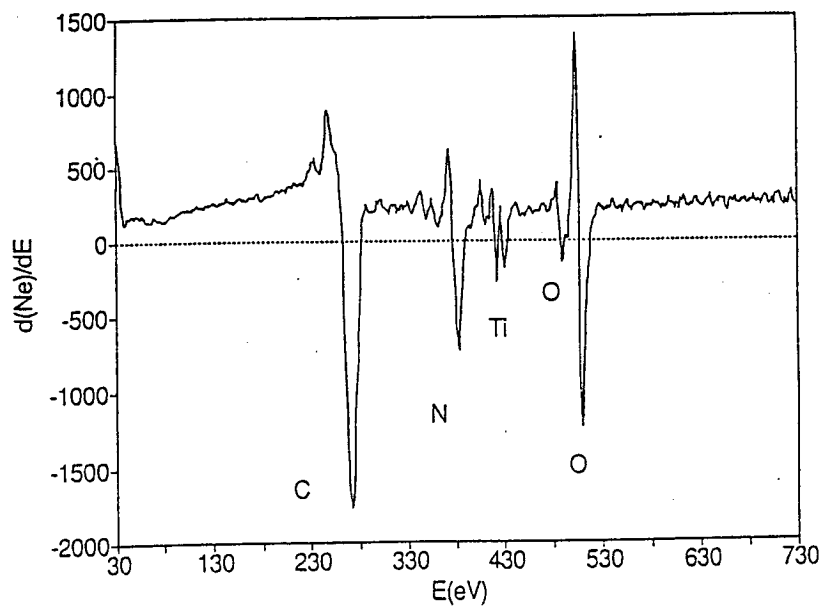

Figure 8.   Rate vs time for pyrrole photocatalyzed oxidation

Figure 9.   Auger spectrum of pyrrole-deactivated catalyst

2. SILICON: DECAMETHYLTETRASILOXANE

The materials of construction for spacecraft components include silicon derived polymers; we take decamethyltetrasiloxane as representative of the volatile siloxane structures which are expected according to Leban and Wagner. This siloxane at feed concentrations of 200 mg/m^3 gave an initial exit concentration of 120 mg/m3 for the 50 mL/min flow and 1000 mg/m^3 water vapor present. No intermediates were detected, and the catalyst deactivated slowly over a 10 hour period, at which time the residual activity was negligible.

The deactivation profile is again linear on a log-log plot (Figure 10), and can be represented by equation (4) below:

rate (t) = rate (initial) / (1. +(time(min))^b)   (4)

where b = 1.07 and time is in minutes.

The total amount of siloxane converted at the time when "total" deactivation was achieved is more than 100 monolayer equivalents of silicon. The Auger spectra of the deactivated catalyst showed titanium, oxygen, carbon, as well as peaks attributed to Si-O bonds and Si-Si bonds. (Figure 11, the tin (Sn) p[eak is produced artificially in preparing the sample for Auger examination))

The conclusions from this segment of the work are as follow:

(i) Silicon, fed as DMTS, deposits irreversibly, along with carbon.

(ii) Nitrogen, fed as indole or pyrrole, deposits irreversibly along with carbon.

(iii) Heteroatom deposition, as indicated by Auger spectroscopy, accompanies and is presumed largely responsible for catalyst deactivation.

(iv) N deposition gives deactivation after a monolayer equivalent of reactant is converted.; silicon only after the order of 100 or more monolayer equivalents.

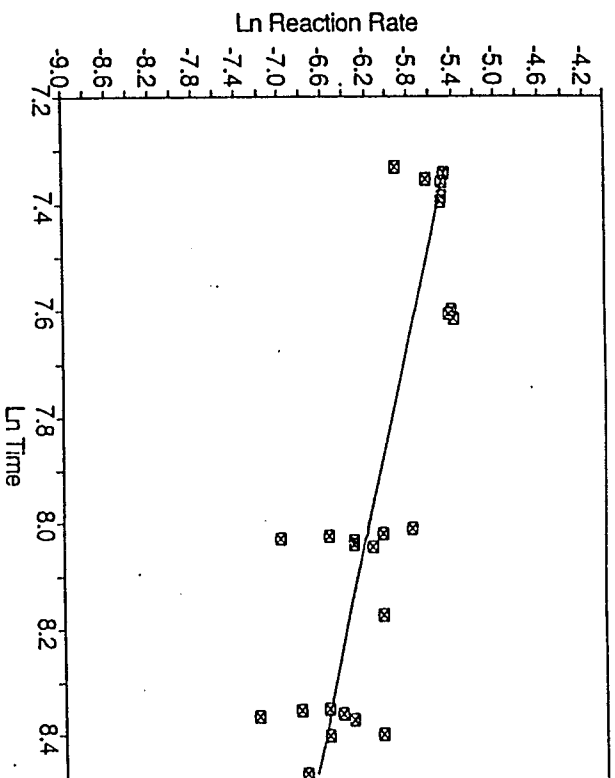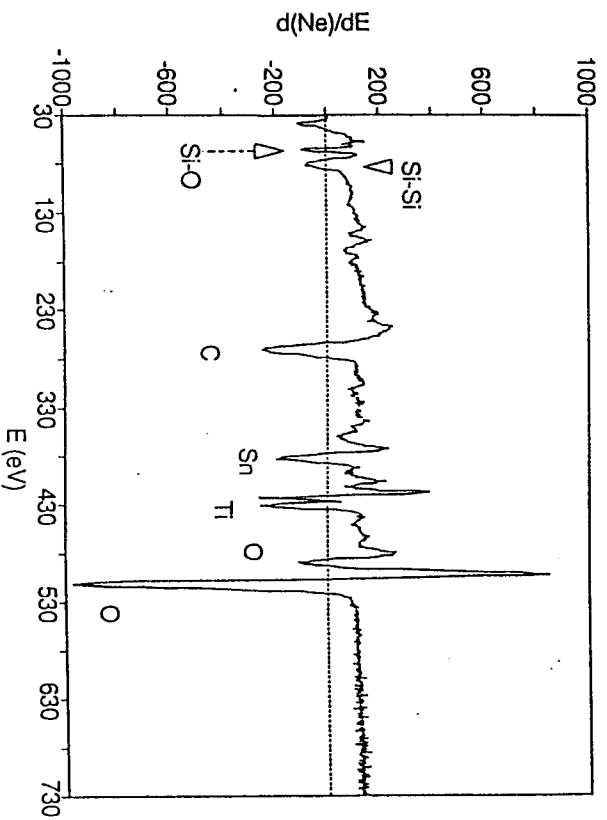(v) The deactivation rate for all three contaminants can be described by equation (4).

Figure 10.   Rate vs. time for decamethyltetrasiloxane oxidation

Figure 11.   Auger spectrum of DMTS-deactivated catalyst.

14

4. REACTOR DESIGN: PHOTOCATALYTIC MONOLITH

The catalytic honeycomb monolith configuration has found widespread application in industry for air treatment, primarily because it provides good gas-solid contacting under laminar flow conditions, thus providing a pressure drop which is one to two orders of magnitude less than experienced with packed bed or fluidized bed catalytic systems. It has additional advantages: in automotive exhaust control, the ceramic honeycomb support can withstand large temperature excursions and still retain form and activity, and in NOx control from power plant exhausts, the monolith can be cast in one meter lengths which can be stacked to create a horizontal "floor" in a vertical exhaust stack.

The monolith also possesses an additional advantage for photocatalysis: the continuous linear channels which completely traverse the monolith leave all inner channel surfaces available for illumination from either end. The monolith can be dip-coated with titanium dioxide aqueous suspensions to provide an optically dense, but thin catalyst film (10-15μm) attached to the monolith walls, thus allowing formation of the photocatalytic monolith configuration.

This configuration has already been recently examined. In parallel with our NASA funded study, begun in 11/90, Suzuki et al at Toyota have briefly reported in 1991 and 1993 on their studies of individual photocatalytic destruction of odor compounds (acetaldehyde, isobutyric acid, toluene, methylmercaptan, hydrogen sulfide, and trimethylamine) in a recirculating reactor configuration. They gave no kinetic equations, but concluded that the compound disappearance followed pseudo-first orfer kinetics. No repeat runs were presented, so deactivation was not explored.

We have completed the first fundamental study of the recirculating, monolith photoreactor and summarize it in section 6. This work includes full mass balances on both gas phase and adsorbed phase reactant and water, and provides satisfying agreement between model and experiment, using acetone conversion as the model conversion. 15

A. FUNDAMENTAL STEADY STATE MODEL

The routine application of photocatalysis to air purification in an enclosed spacecraft is expected to correspond more closely to a steady state, rather than transient, operation. Accordingly, while analysis of the recirculating batch monolith photoreactor, useful in laboratory studies for determination of rate equations and catalyst deactivation, is important fundamentally, the application at hand calls for a steady state analysis, which we have developed for the first time, and summarize in the paragraphs and next two sections below.

A monolith reactor is modeled for ambient temperature removal of trace organic contaminants from air. Using our earlier data and rate equations for acetone and butanol oxidations, we model conversion of these typical contaminants at four different Reynolds numbers using both uniform and non-uniform light intensity profiles within the monolith channels.

For constant assumed light intensity along the channel wall, acetone and butanol concentration profiles have been computed along the monolith channel at Re= 10, 50, 100, and 150. The range of exit diminsionless mixing cup concentrations for acetone is 0.36 to 0.96, Figure 11, which indicates that only in the Re=10 case does the acetone conversion reach more than 50% conversion per single pass. With the more reactive butanol, the model predicts more than 90% conversion in single pass operation even for Reynolds number of 150 (highest gas flow examined). (Figure 12) Acetone oxidations show only small radial gradients, but butanol indicates a faster rate and thus a higher mass transfer influence..

As an example of non-uniform light intensity along the channel walls, a point source lamp located upstream from the monolith entrance is assumed to predict the variable light intensity influence. Calculations indicate that both acetone and 1-butanol are completely oxidized when the point source lamp is placed very close

16

to the monolith entrance, and modest-to-intermediate conversions are obtained for light source placed 10 channel diameters upstream.

These detailed modelling results, including supercomputer use to calculate concentration, velocity and illumination fields, constitute the first and only detailed model of the photocatalytic monolith reactor
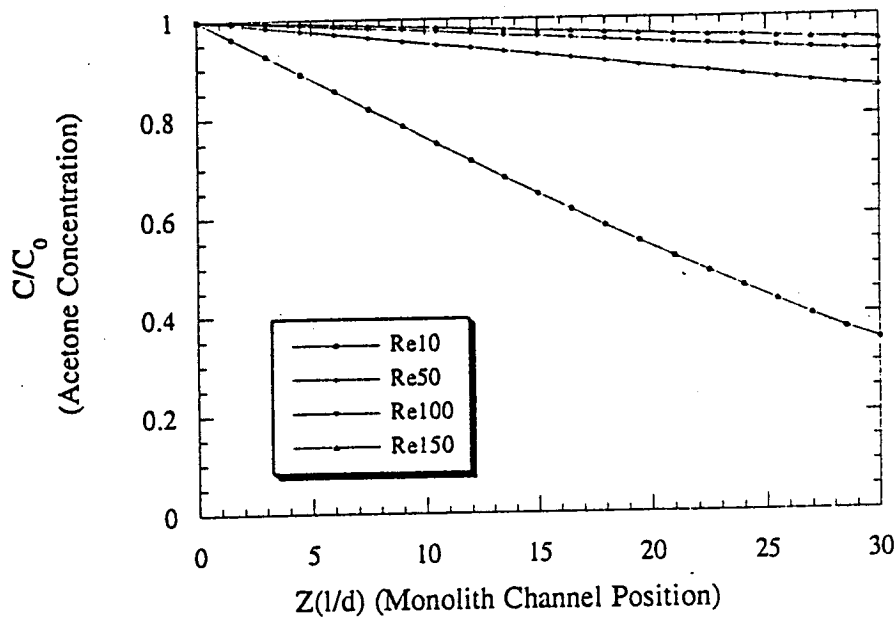
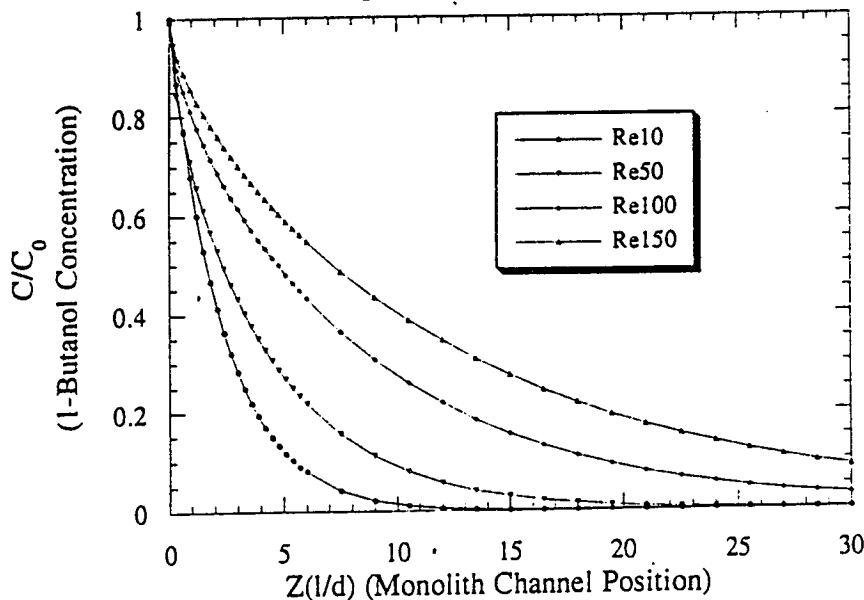Figure 11 Acetone Concentration Profiles for Re=10, 50, 100, 150. (C_0=712.5 mg/m^3, d=0.4 cm)

Figure 12 1-Butanol Concentration Profiles for Re=10, 50, 100, 150. (C_0=121.0 mg/m^3, d=0.4cm)

B. MAXIMUM RATE ASYMPTOTE: THE MASS TRANSFER LIMIT

The maximum possible rate of reaction in any heterogeneous catalytic reactor occurs when the catalyst surface is so active that the reactant concentration is nearly zero at the surface, and we speak of a mass transfer limited rate, because the only resistance to reactant conversion is the convective diffusion transport from the gas phase to the active surface. The calculated mass transfer limited results presented in Figures 13 and 14 below indicate that as Reynolds number increases from slow flow (Re=10) to intermediate flow (Re=150), the increased radial mass transfer brings the butanol conversion performace quite close to the maximum possible rate.

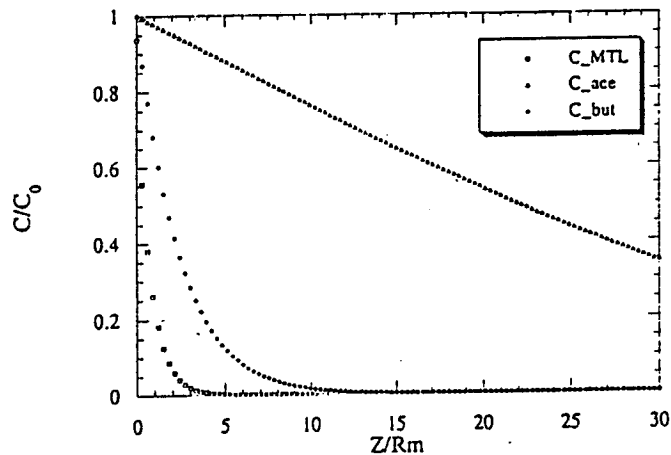Figure 13 Concentration Profiles in Monolith Channel for Re=10
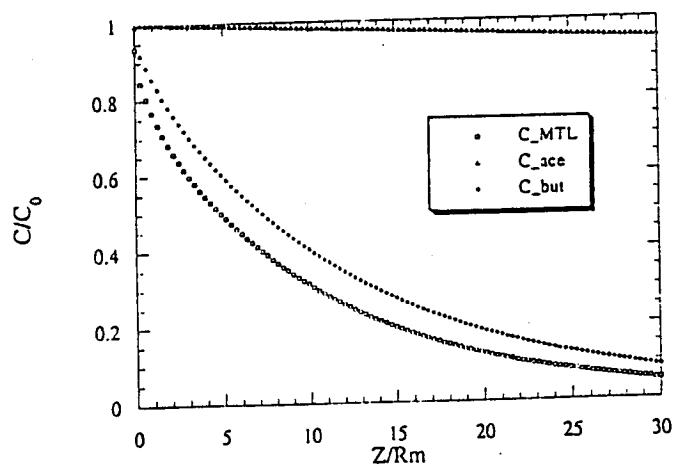(Acetone, 1-Butanol, Mass Transfer Limited Rxn)

Figure 14 - Concentration Profiles in Monolith Channel for Re=150
(Acetone, 1-Butanol, Mass Transfer Limited Rxn)

C. ILLUMINATION DISTRIBUTIONS

The measurement and more realistic calculation of intensity profiles has been accomplished in the following manner:

(a)   A small radiometer is used to measure the distribution across the surface of the emitting light source

(b)   A geometric view factor is calculated (see Figure 15) which requires radial integration acrosss the face of the lamp and uses geometric view factors to calculate the average intensity arriving at any point X along the channel axis.

(c)   The variation in intensity with axial position is calculated, and the difference in total photon rate traversing two nearby channel cross sections is the photon deposition rate on the wall, allowing calculation of the wall intensity as a function of axial position in the monolith.

(d)   The intensity profile along the axis of a channel is measured experimentally by cutting monoliths into lengths of ..25, .50, .75, 1.0, 1.5, 2.0, 3.0, 4,0, 5.0 and 6.0 inches.   The small radiometer sensor is set at the channel exit of each monolith section, and the corresponding experimental intensity falling on that axial position provides the intensity distribution in the six inch monolith reactor.

(e)   The calculated intensity profile from (c) is compared with the measured experimental profile from (d).   The shapes are very similar; however, a correction factor of 0.6 needed to be multiplied times the predicted profile in order to achieve satisfactory agreeement, represented in Figure 16

These results for steady state flow with finite wall rate constants (for acetone and butanol examples), mass transfer limited design (infinite wall rate constants), and intensity field calculation and measurement constitute the complete steady state design characterization of the photocatalytic monolith reactor.
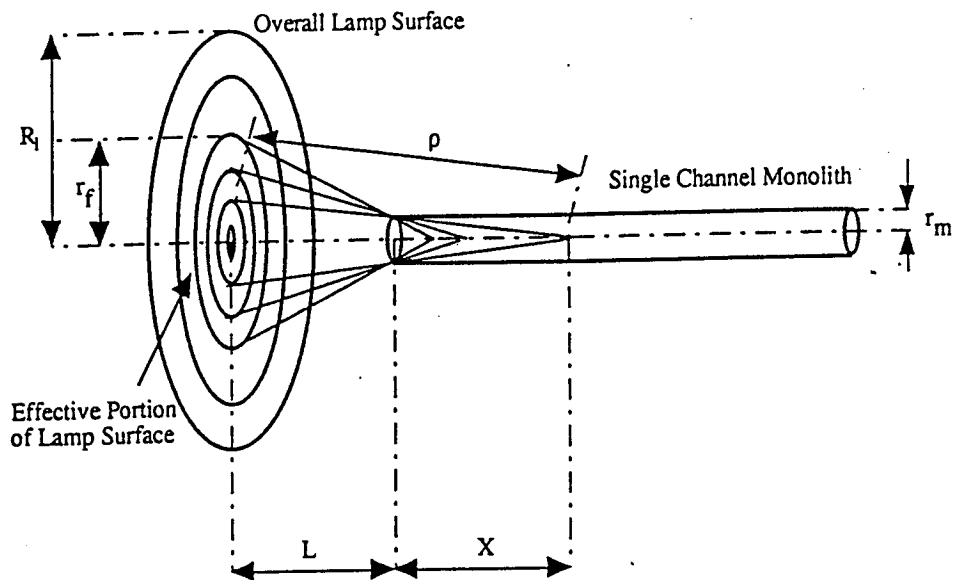
19

Figure 15 Coordinate Illustration for Light Intensity Calculation
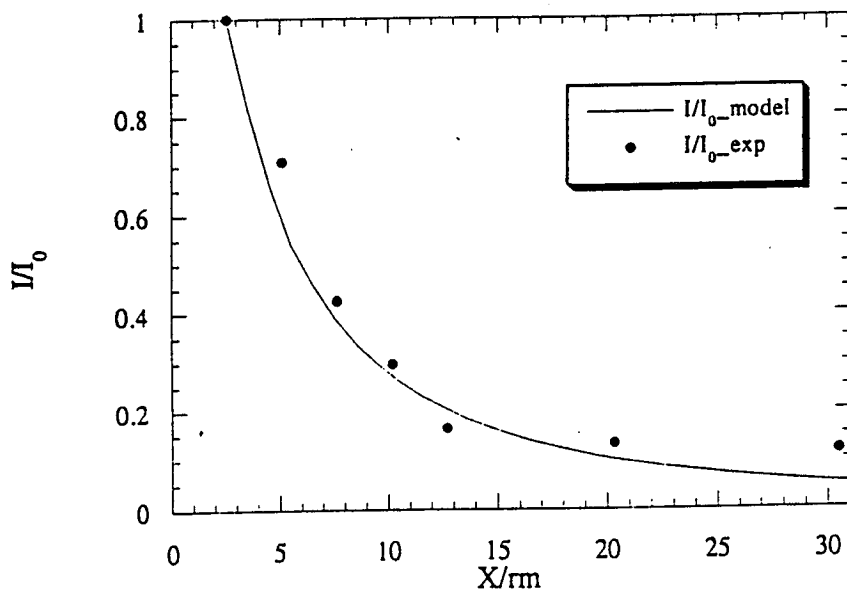

Figure 16 Light Intensity Profile Comparison (1 Lamp Illumination)

5. COMPARATIVE REACTOR DESIGN

A brief comparison of reactor advantages and disadvantages was carried out, involving a fixed bed reactor, fluidized bed reactor, transport (powder) reactor, and monolith reactor. Nothing in this standard comparison of reactor types suggests that the monolith is not the best choice for the application under consideration. (see publication list for reference).

6. MONOLITH EXPERIMENTS AND RECIRCULATING BATCH MODEL: ACETONE CONVERSIONS

Photocatalyzed oxidation of acetone (70-400 mg/m^3) in air was carried out using near-UV illuminated titanium dioxide (anatase form) coated on the surface of a ceramic honeycomb monolith. Considerable adsorption of acetone and water was noted on the catalyst coated monolith; these uptakes were described with a Langmuir adsorption isotherm for acetone and a modified BET adsorption isotherm for water. The acetone photocatalyzed disappearance kinetics on the TiO2 were determined with initial rate differential conversion, recycle reactor data and were analyzed using a Langmuir-Hinshelwood rate form coupled with a reactant mass balance including appreciable acetone monolith adsorption. The model, with parameters evaluated from initial rate data, is then shown to satisfactorily predict reactor behavior at all extents of conversion.

A comparison of the calculated model results, evaluated from initial rate data only, and including adsorption isotherms, and the experimental acetone concentrations in the recirculating reactor, is shown in Figure 16.

Acetone Gas Concentration vs Time

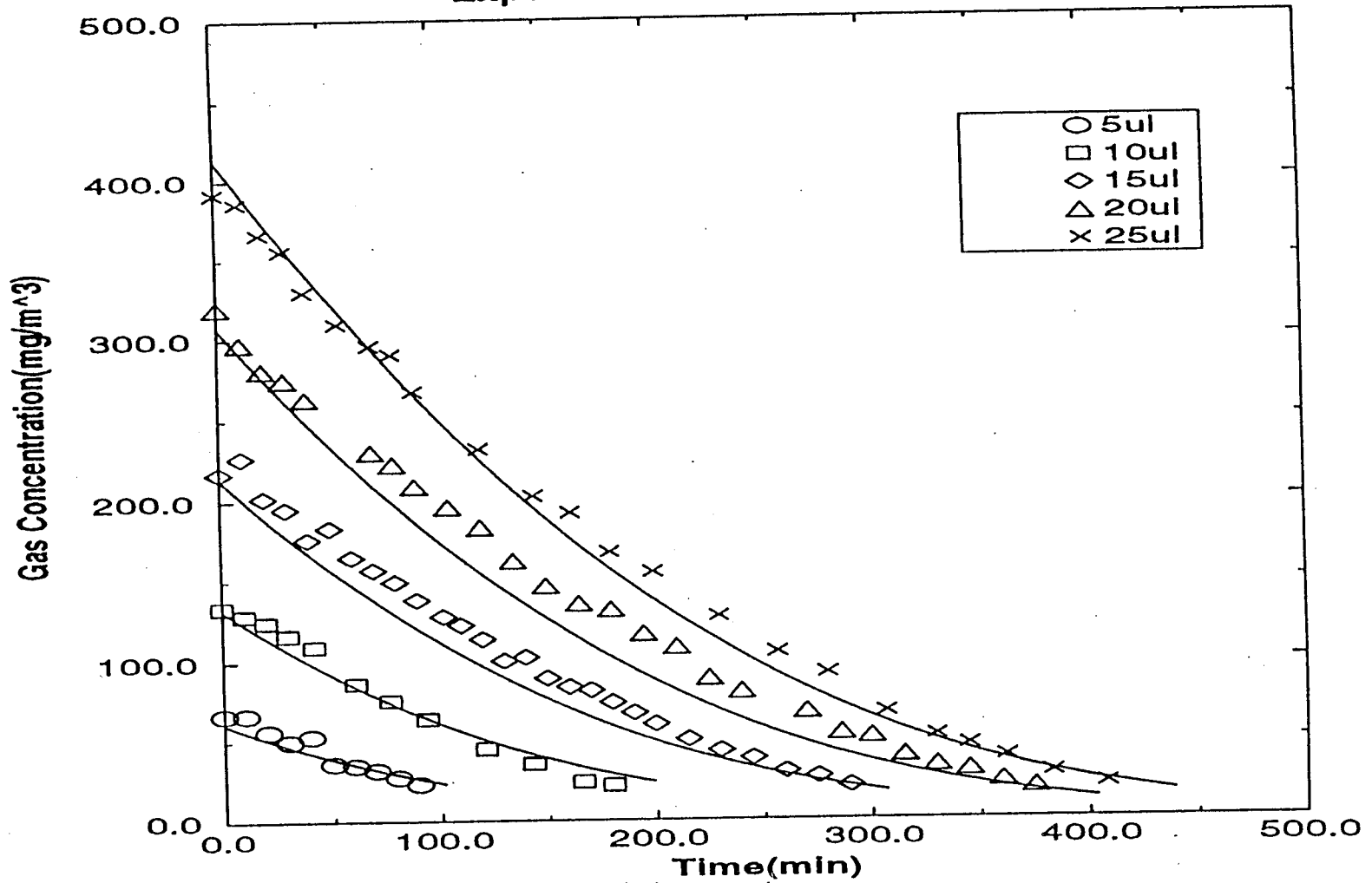## Experiment/Model Comparison

Figure 16

7. HALIDE ENHANCED PHOTOCATALYSIS: ACHIEVEMENT OF 100% CONVERSION

A 1993 report by Berman and Dong noted that the conversion rate of several reactants could be increased by factors of two or three by the addition of appreciable trichloroethylene (TCE) to the feedstream. No rate equations or mechanism were indicated, although the authors suggested that the augmentation could be due to the oxidative attack on the original contaminant by chlorine radicals released during the (chain) reaction conversion of trichloroethylene.

We examined this halide promotion influence, and have demonstrated, for the first time, the achievement of 100% conversion of toluene (modestly reactive by itself) upon TCE addition, provided the toluene level was below about 80 -90 mg/m^3. These remarkable results appear in Figure 17 below. With this novel result, we hope to develop a more active catalyst which can allow rapid conversion of virtually all air contaminants in the Wagner and Leban list.
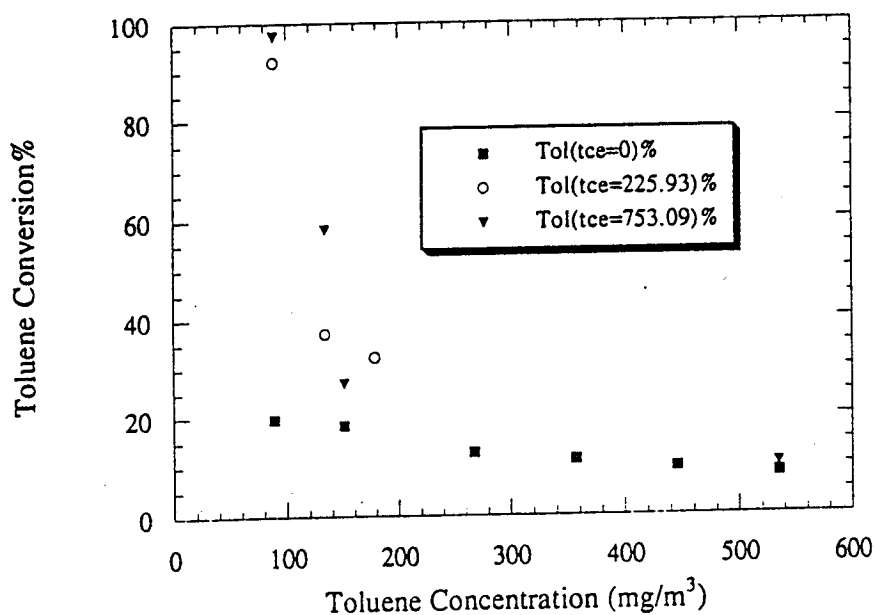

Figure 17 Toluene Conversions with or without TCE

8. PHOTOCATALYST DEACTIVATION

All industrial catalysts have finite lifetimes. The latter may range from as much as one year (or 50,000 miles for automotive exhaust catalysts) to as short as 1-2 seconds, as occurs with acidic cracking catalysts used in petroleum refining. In the latter case, and many others with rapidly deactivating catalysts, catalyst deactivation kinetics and catalyst regeneration schemes are important in establishing the true economic costs, and values added, of heterogeneous catalysts.
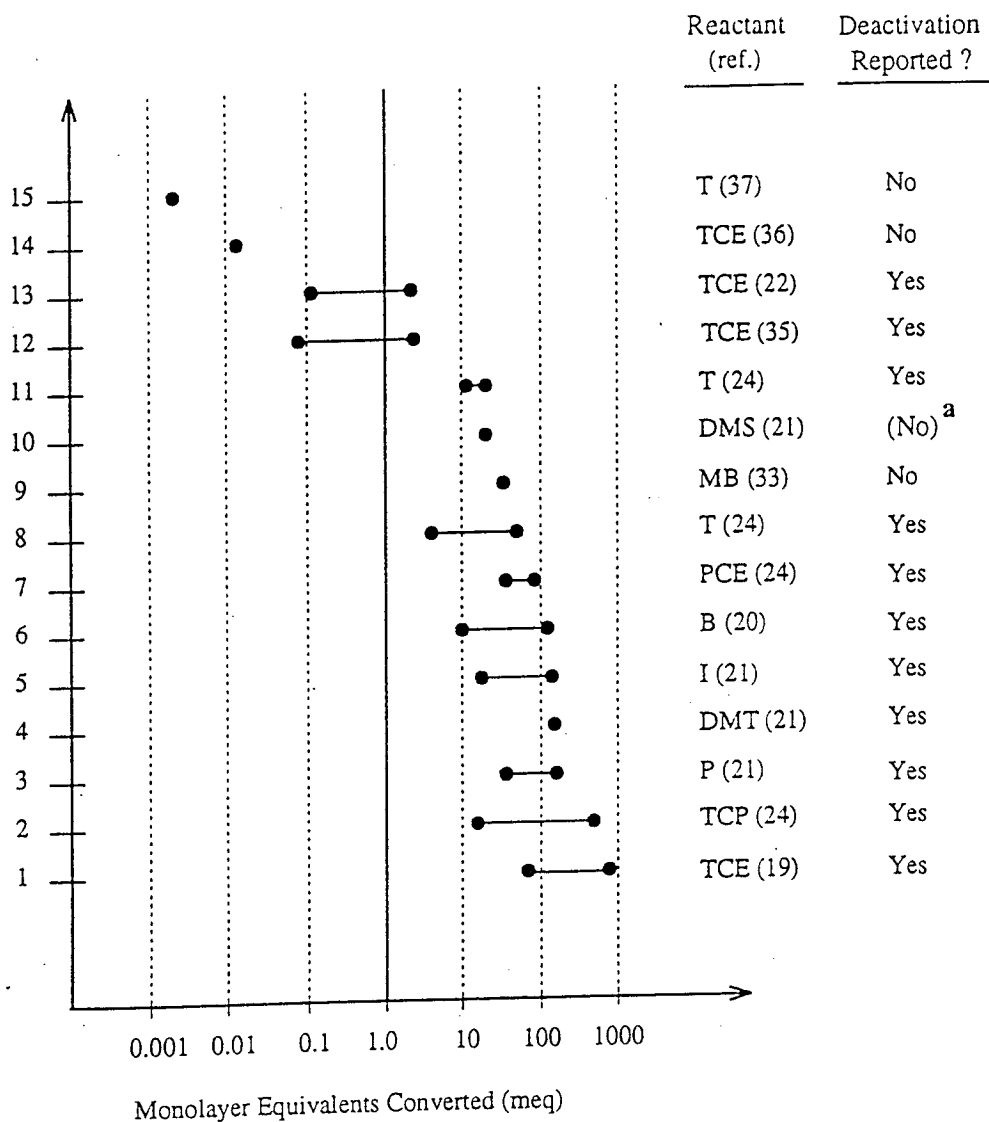
Photocatalysis is a young field, and its workers are only beginning to appreciate that the larger traditions of catalysis include deactivation and regeneration. Most photocatalysis studies to date have not sought to explore the possibility of deactivation, and most papers have not reported it. However, a recent surface science report (Larson and Falconer, Appl. Catal. B, Environ, 4, 325(1994)) demonstrated that a photocatalyst which had deactivated completely during TCE (trichloroethylene) conversion held one to two monolayer-equivalents of carbon on its surface; this carbon desorbed upon heating · ¨primarily in the form of carbon monoxide and carbon dioxide, although its exact form on the catalyst (e.g., carbonate, carboxylate, etc,) is unknown.

This result suggested to us that most catalysts must be deactivating, inasmuch as the penultimate and end products of hydrocarbon contaminant oxidations will all be similar. To establish this premise, we surveyed gas-solid photocatalysis papers, looking for indicators of deactivation, either mentioned by authors (usually parenthetically) or demonstrated in figures or tables even if not mentioned.

This survey established two important points:
(1) for virtually all studies using a single pass reactor, and converting more than 10-100 monolayer equivalents of reactant, deactivation is noticed or present (Figure 18)
(2) in contrast, batch, recirculation reactors show such rapid fall of reactant, and rise and fall of intermediates (if present), that the slower deactivation phenomena is not evident, even if present.

23

Reactant (ref.)	Deactivation Reported ?
T (37)	No
TCE (36)	No
TCE (22)	Yes
TCE (35)	Yes
T (24)	Yes
DMS (21)	(No)[a]
MB (33)	No
T (24)	Yes
PCE (24)	Yes
B (20)	Yes
I (21)	Yes
DMT (21)	Yes
P (21)	Yes
TCP (24)	Yes
TCE (19)	Yes

Monolayer Equivalents Converted (meq)

[a] *Deactivation was not reported, but was evident upon review of the data.*

Figure 18: Data summary demonstrating that photocatalyst deactivation is observed or recorded for all reports where more than 100 monolayer equivalents of contaminant were reacted.

24

The importance of deactivation being established, there remains the task of identifying regeneration schemes. Here the literature is very sparse, but the few examples found suggest logical avenues for work:

(i) isolation in air for short periods, in the dark or under illumination, and

(2) short term mild heating to react off residual carbon.

This areas will be pursued in our laboratory under other support.

9. MULTICOMPONENT CONTAMINANT CONVERSIONS

Multicomponent conversions in catalysis usually exhibit mutual rate inhibition, due to the competiton among reactants (air contaminants in this case) for a finite number of catalyst surface sites. We have found .(M. Sauer, PhD thesis, 1995) that, for example, the simultaneous conversion of acetone and butanol causes such a mutual inhibition or rate slowing, with the less strongly held acetone not beginning to react appreciably until most of the more strongly held alcohol was converted.

A first successful model of multicomponent photocatalysis was created by Sauer in our lab (J. Catalysis, **158**, 570 (1996)) under other support. This model accounted for the conversion of a single contaminant, ethanol, through a pathway of intermediates including acetaldehyde, acetic acid, formaldehyde, formic acid, and carbon dioxide. The reaction model was applied to the monolith configuration developed with our NASA support, and shown to adequately describe the behavior of a recirculating, batch reactor.

We have sought to enhance the basis for reactor design when rate enhancement, as well as inhibition, is present. To this end, we have analyzed and established a kinetic model for the halide enhancement(section 7) as a function of a reactor design variable, the intensity of the illuminating light. (Upadhya and Ollis, J. Adv. Oxidation Technol. (submitted)). This analysis rationalizes the observed behavior (Figure 19) showing that the rate dependence on intensity can vary from first to one half order when the concentration of reactant is changed from a high value to a low value.
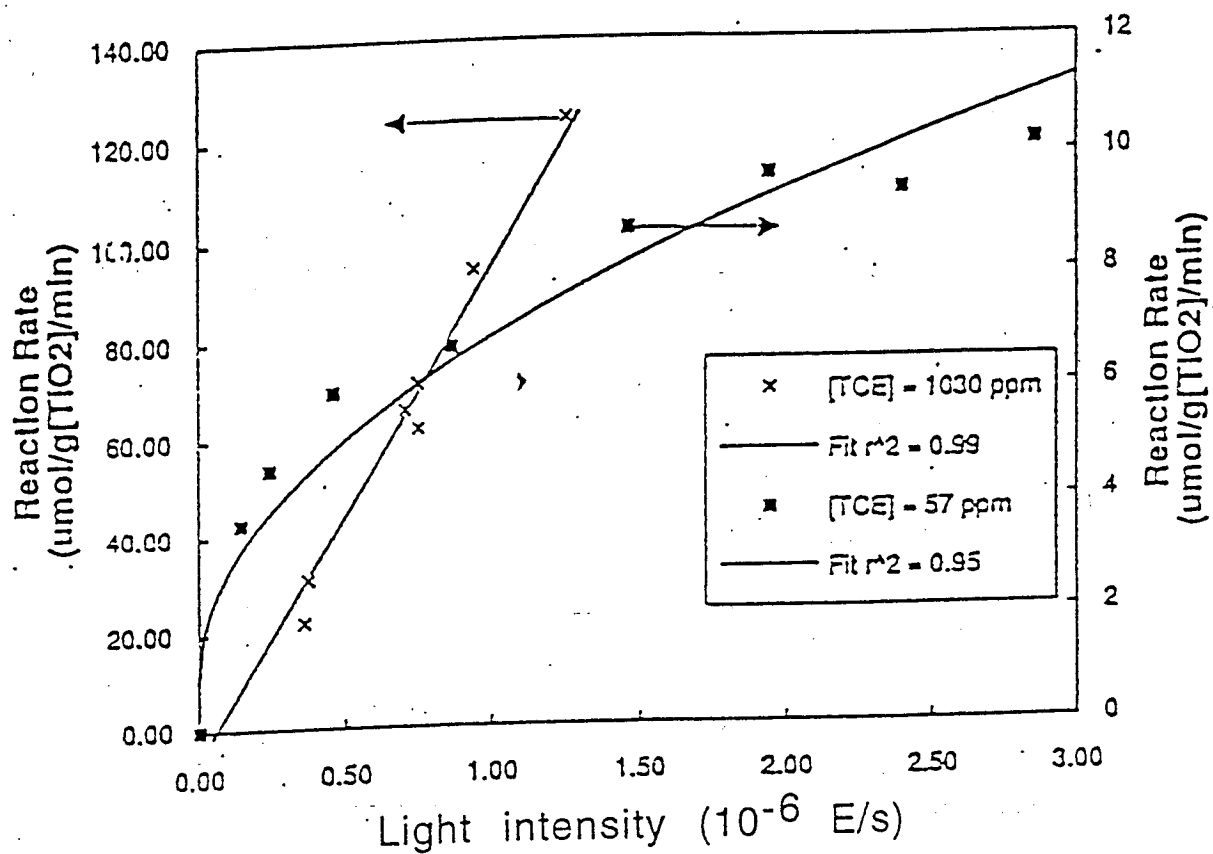
Figure 19: TCE photocatalytic rate vs. light intensity. Rate is linear in intensity at high (1030 ppmv) concentration, but varies as square root of intensity at low (57 ppmv) concentration (Nimlos et al, Environ. Sci., Tech., **27**, 732, 1993.

10. CONCLUSIONS

In the course of our NASA grant NAG 2-684, we have accomplished the followiing milestones:

(1) constructed a powder layer downflow photocatalytic reactor and used it to ascertain the conversion kinetics of acetone, butanol, buteraldehyde, and m-xylene, all expected contaminants in spacecraft air.

(2) Examined catalyst deactivation rates for the first time by conversion of expected contaminants which contain heteroatoms N, Si, or S. The nitrogen compounds cause catalyst deactivation and thus are most problematic, the silicon compounds much less so, and the dimethylsufide studied was relatively unreactive and did not deactivate the catalyst.

(3) Constructed reactor engineering models for the steady state photocatalytic monolith for pertinent cases of a constant wall illumination, point source illumination, variable flow rates, weakly (acetone) to moderately (butanol) to infinitely (mass transfer limit) reactive contaminants, and ascertained the illumination fields within the photocatalytic monolith, all for the first time.

(4) Constructed and verified an engineering design model for a batch recirvulating monolith reactor of the configuration first explored in a 1991 experimental study by Toyota. This recirculating system is a small scale mimic of a recirculating ventilation and air treatment system in a spacecraft.

(5) Demonstrated for the first time the achievement of 100% conversion of an aromatic hydrocarbon by the addition of trichloroethylene. This halide "promotion" effect may open the door to development of the next generation of more active photocatalysts.

(6) Demonstrated with our own data and that of others that photocatalyst deactivation does occur, and that this evolving and promising field needs to place catalyst deactivation and regeneration kinetics and procedures on a quantitative footing.

(7) Demonstrated a multicomponent model, the first to appear, for the serial, simultaneous conversion of a single contaminant and all its intermediates, to carbon dioxide final product. Our successful approach establishes the basis for development of a multicomponent contaminant model, which will provide the design basis for spacraft air cleaning.

11. LIST OF PUBLICATIONS

1   "Heterogeneous Photocatalytic Oxidation of Gas-Phase Organics for Air Purification: Acetone, 1-Butanol, Buteraldehyde, Formaldehyde, and m-Xylene Oxidation", J. Peral, and D. F. Ollis, Journal of Catalysis, 136, 554, (1992).

2.   Photocatalytic Purification and Treatment of Water and Air, D. F. Ollis and H. Al-Ekabi(editors), Elsevier, Amsterdam, 1993, 816 pp.

3.   "Photoreactors for Purification and Decontamination of Air", D. F. Ollis, in Photocatalytic Purification and Treatment of Water and Air, D. F. Ollis and H. Al-Ekabi(editors), Elsevier, Amsterdam, 1993, 816 pp.

4.   "Photocatalyst Deactivation: Oxidation of Decamethyl-tetra-siloxane, Pyrrole, Indole, and Dimethyl Sulfide", J. Peral and D. F. Ollis, in Photocatalytic Purification and Treatement of Water and Air, D. F. Ollis and H. Al-Ekabi(editors), Elsevier, Amsterdam, 1993, 816 pp.

5.   "Photocatalytic Monolith Reactor Analysis", Y. Luo and D. F. Ollis, Chemical Engineering Communications (submitted)(1997).

6.   "Acetone Oxidation in a Photocatalytic Monolith Reactor", M. Sauer and D. F. Ollis, J. Catalysis, **149**, 81, 1994.

7.   "Heterogeneous Photocatalytic Oxidation of Trichloroethylene and Toluene Mixtures in Air", Y. Luo and D. F. Ollis, J. Catalysis, **163**, 1, 1996.

8.   "On the Simultaneous Intensity and Concentration Dependence of Trichloroethylene Photocatalyzed Oxidation:" S. Upadhya and D. F. Ollis, J. Adv. Oxidation Technologies, (submitted, 1997)

12. LIST OF PRESENTATIONS

1. "Photocatalytic Air Purification", J. Peral and D. F. Ollis, AIChE meeting, Minneapolis, MN, August, 1991.

2. "Photocatalytic Air Purification", ACS meeting, San Francisco, CA, April 1992.

3. "Photocatalytic Air Purification", J. Peral and D. F. Ollis, NASA-Langley, Hampton, VA, October, 1991.

4. "Photocatalytic Reactors for Purification and Decontamination of Air", D. F. Ollis, Intl. Conf on Photocatalytic Purification and Treatment of Water and Air, London, Ontario, Canada, Nov. 1992

5. "Photocatalyst Deactivation: Oxidation of Decamethyl-tetrasiloxane, Pyrrole, Indole, and Dimethylsulfide", J. Peral and D. F. Ollis, (conference in ref. #4).

6. "Photocatalysis for Air Purification and Recycle", US/Russia NSF Symposium on Environmental Catalysis, January 14-16, 1994, Wilmington, DE.

7. "Photocatalytic Oxidation of Acetone in a Monolith Reactor". M. Sauer and D. F. Ollis, AIChE mtg, August,1993, Minneapolis, MN.

8-9. "Photocatalytic Oxidation of Ethanol in a Monolith Reactor: Kinetics and Reactor Models" M. Sauer and D. F. Ollis, AIChE mtg, Denver, CO, August, 1994 and National Renewable Energy Laboratory, Golden CO, August, 1994.

10-11. "Photocatalyzed Conversions of Toluene/Trichloroethylene Mixtures in Air", Y. Luo and D. F. Ollis, AIChE mtg, August, Denver, CO and National Renewable Energy Laboratory, Golden CO, August, 1994.

12. LIST OF PRESENTATIONS (continued)

12. "Photocatalytic Air Purification", EPA, Research Triangle Park, NC, May, 1995.

13. "Photocatalytic Air Purification: Progress, Problems, Prospects", World Environmental Congress, London. Ontario, Canada, September, 1995.

14. "Photocatalytic Air Purification: Halide Enhancement", NREL, Golden, CO, October, 19995.

15. "On the Simultaneous Concentration and Intensity Dependence of Reaction Rate during Photocatalytic Oxidation of Trichloroethylene", S. Upadhya and D. F. Ollis, 2nd International Conference on TiO2 Photocatalysis, Cincinnati, OH, October, 1996.

16. "Halide Enhanced Photocatalysis", O. d'Hennezel and D. F. Ollis, 2nd International Conference on TiO2 Photocatalysis, Cincinnati, OH, October, 1996.

13. LIST OF RESEARCH PARTICIPANTS

Dr. Jose Peral (postodoctoral), Department of Chemistry, University of Barcelona, Spain, 11/90-9/92

Yang Luo (PhD, 7/94), Department of Chemical Engineering, North Carolina State University, 6/91-7/94); currently at International Paper, Erie Research lab, Erie, Pennsylvania.

Michael Sauer (PhD, 6/95), North Carolina State University.

Santosh Upadhya (MS 6/96), North Carolina State University; currently project engineer, Santa Clara Valley, CA.